Available online at www.sciencedirect.com
ScienceDirect
European Journal of Mechanics B/Fluids 28 (2009) 72–87

Interactive boundary layer models for channel flow

J. Cousteix [a,b,*], J. Mauss [c]

[a] *Département Modèles pour l'Aérodynamique et l'Énergétique, ONERA, 2 avenue Édouard Belin, B.P. 4025, 31055 Toulouse Cedex 4, France*
[b] *École Nationale Supérieure de l'Aéronautique et de l'Espace, 10, avenue Édouard Belin, 31055 Toulouse Cedex, France*
[c] *Institut de Mécanique des Fluides de Toulouse, UMR-CNRS and Université Paul Sabatier, 118, route de Narbonne, 31062 Toulouse Cedex, France*

Received 19 March 2007; received in revised form 21 September 2007; accepted 16 January 2008

Available online 16 February 2008

Abstract

In this paper, the aim is to present the results of a new approach for the asymptotic modeling of two-dimensional steady, incompressible, laminar flows in a channel. More precisely, for high Reynolds numbers, the walls of the channel are deformed in such a way that separation is possible. Of course, numerical solutions of Navier–Stokes equations can be calculated but it is believed that an asymptotic analysis helps in the understanding of the flow structure. Numerical solutions of Navier–Stokes equations are compared with solutions of asymptotic models included in a more general model called global interactive boundary layer.

Keywords: Interactive boundary layer; Separation; Channel flow; Asymptotic analysis

1. Introduction

In the study of high Reynolds number flows past a solid wall [1,2], Navier–Stokes equations reduce formally to Euler equations far from the walls. Near the walls, the corresponding inviscid approximation is corrected by a boundary layer solution which takes into account viscosity effects. The standard approach is hierarchical in the sense that the inviscid solution is calculated independently from the viscous solution and then the boundary layer effects are introduced.

Here, we consider a steady, two-dimensional, incompressible, laminar flow in a channel with small wall perturbations. These perturbations, such as indentations, are sufficiently significant to produce streamwise adverse pressure gradients which cannot be neglected. Physical phenomena such as flow separation or upstream influence cannot be described by following the standard approach.

The hierarchy introduced in the standard theory and according to which the knowledge of the inviscid solution enables us to calculate the boundary layer is broken. A strong coupling between the viscous and inviscid zones takes place.

Then, the alternative is either to solve the complete Navier–Stokes equations or to find simpler models in which the boundary layer and Euler equations are no longer hierarchized. These models form the Interactive Boundary Layer

* Corresponding author.
E-mail addresses: Jean.Cousteix@onecert.fr (J. Cousteix), mauss@cict.fr (J. Mauss).

0997-7546/$ – see front matter
doi:10.1016/j.euromechflu.2008.01.003

theory, IBL. The analysis of IBL models leads to a better understanding of the flow structure and of the corresponding significant scales.

The mathematical justification of IBL is the asymptotic analysis but we are faced to a paradox since, formally, when the study is carried out for a Reynolds number tending to infinity, the hierarchy imposes itself in a natural way. Essentially, this is the result of the construction process of the asymptotic expansions which leads to expansions of Poincaré type called regular expansions. With regular expansions, the paradox is apparently broken if it is possible to match directly the component of velocity normal to the wall between the viscous and "inviscid" zones. In external flows, the triple deck theory answers these questions [8–10,17]. For channel flows, the counterpart of the triple deck theory has been established by Smith [13,14]. However, these theories introduced very restricting hypotheses on the scales of the flow.

In order to overcome these limitations, it is much better to use generalized expansions which are such that a small parameter of the problem can be present in the functions constituting the expansions. Then, the inverse of the Reynolds number and the thickness ε of the boundary layer may not be linked so tightly and may not be so small as in Smith's theory. In this way, we can take into account effects which are no longer considered as being of second order.

Two methods can be used. In the first one, different domains are considered. In one domain, the Euler equations are valid and in the other ones the boundary layer equations apply. Obviously, the Eulerian zone is not exactly inviscid because, in the case of strong coupling, the effects of viscosity must be represented which is not possible with regular expansions. These methods are generalizations of the method of asymptotic expansions with a matching principle called modified Van Dyke's principle [2].

In the second method, the flow is analyzed with the Successive Complementary Expansion Method, SCEM, in which we seek a uniformly valid approximation in the whole domain. Thanks to generalized expansions, the effect of the boundary layer on the Eulerian region and the reciprocal effect are considered simultaneously. This method, developed by Cousteix and Mauss [1,2] is based upon the idea that the reasoning used in the method of matched asymptotic expansions must be inverted. A structure of a uniformly valid expansion is assumed and then the method of construction is deduced. If we know that the flow is well approximated by a solution of Euler equations in a certain domain, the question is to determine what must be added to obtain a uniformly valid approximation of the solution of Navier–Stokes equations. This method has been used by Dechaume et al. [4] to calculate channel flows with small wall deformations.

More precisely, in a channel, there is no external flow region and the asymptotic models for the flow perturbations are mainly based on an inviscid rotational core flow region together with boundary layers near the walls. The asymptotic analysis of these flows has been performed essentially by Smith [13–15] and a systematic approach has been proposed later by Saintlos and Mauss [12]. A comprehensive discussion of this structure can be found in Sobey [16]. The modelling of channel flow has also been examined by Lagrée et al. [5] and by Lagrée and Lorthois [6] who consider in particular the flow in axisymmetric pipes.

In the present paper, the formulation of the problem includes two parameters, the Reynolds number $\mathcal{R}$ and the thickness ε of the boundary layer generated by the walls indentations (Section 2). A consistent model is obtained by coupling Euler equations, valid in the flow core for large Reynolds numbers, and Prandtl equations, valid in the whole field for small values of ε (Sections 3–5). The interaction between the two sets of equations is primarily based on the pressure. In Section 6, a simplified method for the pressure calculation is obtained for a class of indentations which contains the critical case of Smith's theory. Results are compared with those obtained from a numerical solution of Navier–Stokes equations. Another method for calculating the pressure is based on the linearized form of a more complete model. The formulation of the model, its numerical solution and results are given in Section 7.

2. Formulation of the problem

Dimensionless Navier–Stokes equations can be written

$$\mathbf{div}\,\vec{V} = 0, \quad (\mathbf{grad}\,\vec{V})\cdot\vec{V} = -\,\mathbf{grad}\,\Pi + \frac{1}{\mathcal{R}}\Delta\vec{V} \tag{1}$$

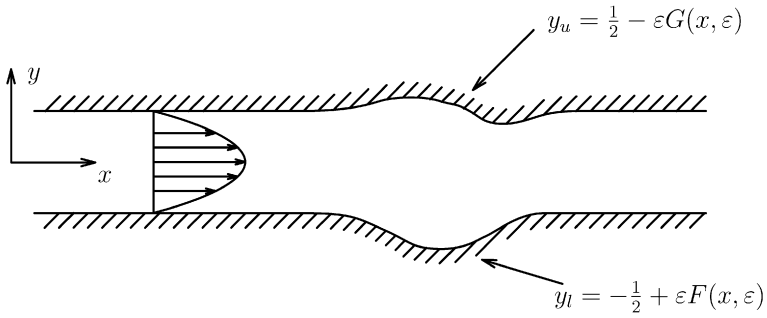

Fig. 1. Flow in a two-dimensional channel with deformed walls. In this figure, all quantities are dimensionless.

where $\mathcal{R}$ is the Reynolds number. The above equations are written in an orthonormal axis-system. Coordinates x and y are reduced by the width H^* of the basic channel whose lower wall is $y = -\frac{1}{2}$ and upper wall is $y = \frac{1}{2}$ (Fig. 1). The velocity components are reduced by a reference velocity V^* defined below by (3). The Reynolds number is

$$\mathcal{R} = \frac{\varrho^* V^* H^*}{\mu^*} \tag{2}$$

where ϱ^*, V^*, H^* and μ^* are dimensionalized quantities denoting the density, the reference velocity, the width of the basic channel and the viscosity coefficient.

The reference velocity V^* is expressed as a function of the basic pressure gradient or, equivalently, of the dimensionalized mass flow $\mathcal{Q}^*$ per unit width of the channel

$$\mathcal{Q}^* = \varrho^* V^* H^* \int_{-1/2}^{1/2} u_0 \,\mathrm{d}y, \quad V^* = 6\frac{\mathcal{Q}^*}{\varrho^* H^*}, \quad \frac{\mathrm{d}\Pi_0}{\mathrm{d}x} = -\frac{2\mu^*}{\varrho^* V^* H^*} \tag{3}$$

where the basic plane Poiseuille flow is

$$u_0 = \frac{1}{4} - y^2, \quad v_0 = 0, \quad \Pi_0 = -\frac{2x}{\mathcal{R}} + p_0 \tag{4}$$

and p_0 is an arbitrary constant.

The flow is perturbed by indentations of the lower and upper walls

$$y_l = -\frac{1}{2} + \varepsilon F(x,\varepsilon), \qquad y_u = \frac{1}{2} - \varepsilon G(x,\varepsilon) \tag{5}$$

where ε is a small parameter (Fig. 1). As shown in Section 3, a significant perturbation is obtained if we seek a solution in the form of generalized expansions

$$v_{(x)} = u_0(y) + \varepsilon u(x,y,\varepsilon), \quad v_{(y)} = \varepsilon v(x,y,\varepsilon), \quad \Pi - p_0 = -\frac{2x}{\mathcal{R}} + \varepsilon p(x,y,\varepsilon) \tag{6}$$

where (u, v, p) denote the characteristics of the flow perturbation. The Navier–Stokes equations become

$$\frac{\partial u}{\partial x} + \frac{\partial v}{\partial y} = 0 \tag{7a}$$

$$\varepsilon\left(u\frac{\partial u}{\partial x} + v\frac{\partial u}{\partial y}\right) + u_0\frac{\partial u}{\partial x} + v\frac{\mathrm{d}u_0}{\mathrm{d}y} = -\frac{\partial p}{\partial x} + \frac{1}{\mathcal{R}}\left(\frac{\partial^2 u}{\partial x^2} + \frac{\partial^2 u}{\partial y^2}\right) \tag{7b}$$

$$\varepsilon\left(u\frac{\partial v}{\partial x} + v\frac{\partial v}{\partial y}\right) + u_0\frac{\partial v}{\partial x} = -\frac{\partial p}{\partial y} + \frac{1}{\mathcal{R}}\left(\frac{\partial^2 v}{\partial x^2} + \frac{\partial^2 v}{\partial y^2}\right) \tag{7c}$$

For high Reynolds numbers, the reduced equations obtained by taking the limit form for $\mathcal{R} \to \infty$ are of first order leading to a singular perturbation.

In the core flow, we are looking for approximations such as

$$u = u_1(x,y,\varepsilon) + \cdots, \quad v = v_1(x,y,\varepsilon) + \cdots, \quad p = p_1(x,y,\varepsilon) + \cdots \tag{8}$$

Formally, neglecting terms of order $O(1/\mathcal{R})$, for the core flow, we obtain the nonlinear set of equations

$$\frac{\partial u_1}{\partial x} + \frac{\partial v_1}{\partial y} = 0 \tag{9a}$$

$$\varepsilon\left(u_1\frac{\partial u_1}{\partial x} + v_1\frac{\partial u_1}{\partial y}\right) + u_0\frac{\partial u_1}{\partial x} + v_1\frac{\mathrm{d}u_0}{\mathrm{d}y} = -\frac{\partial p_1}{\partial x} \tag{9b}$$

$$\varepsilon\left(u_1\frac{\partial v_1}{\partial x} + v_1\frac{\partial v_1}{\partial y}\right) + u_0\frac{\partial v_1}{\partial x} = -\frac{\partial p_1}{\partial y} \tag{9c}$$

If, in addition, terms of order $O(\varepsilon)$ are neglected, we obtain the linear equations

$$\frac{\partial u_1}{\partial x} + \frac{\partial v_1}{\partial y} = 0 \tag{10a}$$

$$u_0\frac{\partial u_1}{\partial x} + v_1\frac{\mathrm{d}u_0}{\mathrm{d}y} = -\frac{\partial p_1}{\partial x} \tag{10b}$$

$$u_0\frac{\partial v_1}{\partial x} = -\frac{\partial p_1}{\partial y} \tag{10c}$$

It is useful to note the behaviour of the solution of (10a)–(10c) in the vicinity of the walls. For instance, as $y \to -1/2$, we have

$$u_1 = -2p_{10}\ln\left|\frac{1}{2} + y\right| + c_{10} + \cdots \tag{11a}$$

$$v_1 = -p_{10x} + 2p_{10x}\left(\frac{1}{2} + y\right)\ln\left|\frac{1}{2} + y\right| - \left(\frac{1}{2} + y\right)(2p_{10x} + c_{10x}) + \cdots \tag{11b}$$

$$p_1 = p_{10} + \frac{1}{2}\left(\frac{1}{2} + y\right)^2 p_{10xx} + \cdots \tag{11c}$$

In the above equations, p_{10} and c_{10} are functions of x and ε. The letter x in index denotes a derivative with respect to the streamwise variable x.

3. Uniformly valid approximation

In order to satisfy the no-slip condition at the walls, two boundary layers are introduced in which the appropriate variables are

$$Y = \frac{\frac{1}{2} + y}{\varepsilon}, \qquad \widehat{Y} = \frac{\frac{1}{2} - y}{\varepsilon} \tag{12}$$

In terms of boundary layer variables, the boundary layer thicknesses are of order 1. Then, in the two boundary layers, we have $u_0 = O(\varepsilon)$. In this way, u_0 and εu are of the same order near the walls. The velocity $u_0 + \varepsilon u$ in (6) can be negative and the approximation is said significant. According to SCEM [2], a uniformly valid approximation is obtained by complementing the core approximation

$$u = U_1(x, Y, \varepsilon) + \widehat{U}_1(x, \widehat{Y}, \varepsilon) + u_1(x, y, \varepsilon) \tag{13a}$$

$$v = \varepsilon V_1(x, Y, \varepsilon) - \varepsilon\widehat{V}_1(x, \widehat{Y}, \varepsilon) + v_1(x, y, \varepsilon) \tag{13b}$$

$$p = \Delta(\varepsilon)P_1(x, Y, \varepsilon) + \Delta(\varepsilon)\widehat{P}_1(x, \widehat{Y}, \varepsilon) + p_1(x, y, \varepsilon) \tag{13c}$$

where the gauge function $\Delta(\varepsilon)$ is yet undetermined. Here, the quantities (u, v, p) do not represent any more the exact solution but only an approximate solution.

The form of approximation for v in (13b) is imposed by the continuity equation which must be nontrivial even in the boundary layers

$$\frac{\partial U_1}{\partial x} + \frac{\partial V_1}{\partial Y} = 0, \qquad \frac{\partial \widehat{U}_1}{\partial x} + \frac{\partial \widehat{V}_1}{\partial \widehat{Y}} = 0 \tag{14}$$

With this formulation, it is clear that, as (u_1, v_1) represent an approximation in the core of the flow, we have

$$Y \to \infty: \quad U_1 \to 0, \quad V_1 \to 0 \tag{15a}$$

$$\widehat{Y} \to \infty: \quad \widehat{U}_1 \to 0, \quad \widehat{V}_1 \to 0 \tag{15b}$$

Along the walls $Y = F(x, \varepsilon)$ and $\widehat{Y} = G(x, \varepsilon)$, the condition of zero velocity associated to the approximation (13a)–(13b) yields

$$Y = F(x, \varepsilon): \quad u_0 + \varepsilon U_1 + \varepsilon u_1 = 0, \quad \varepsilon V_1 + v_1 = 0 \tag{16a}$$

$$\widehat{Y} = G(x, \varepsilon): \quad u_0 + \varepsilon \widehat{U}_1 + \varepsilon u_1 = 0, \quad -\varepsilon \widehat{V}_1 + v_1 = 0 \tag{16b}$$

4. IBL model for the lower wall

In order to obtain a uniformly valid approximation covering the lower boundary layer and the core flow, we set

$$u = U_1(x, Y, \varepsilon) + u_1(x, y, \varepsilon) \tag{17a}$$

$$v = \varepsilon V_1(x, Y, \varepsilon) + v_1(x, y, \varepsilon) \tag{17b}$$

$$p = \Delta(\varepsilon) P_1(x, Y, \varepsilon) + p_1(x, y, \varepsilon) \tag{17c}$$

where, for the sake of simplicity of notation, the same notation (u, v, p) as for the preceding approximation given by (13a)–(13c) is used. The inertia and the viscous terms have the same order in the boundary layer if we take formally

$$\mathcal{R} = \mathrm{O}\left(\frac{1}{\varepsilon^3}\right) \tag{18}$$

and the Navier–Stokes equations become

$$\frac{\partial U_1}{\partial x} + \frac{\partial V_1}{\partial Y} = 0 \tag{19a}$$

$$\begin{aligned} &\varepsilon\left[(U_1 + u_1)\left(\frac{\partial U_1}{\partial x} + \frac{\partial u_1}{\partial x}\right) + (\varepsilon V_1 + v_1)\left(\varepsilon^{-1}\frac{\partial U_1}{\partial Y} + \frac{\partial u_1}{\partial y}\right)\right] + u_0\left(\frac{\partial U_1}{\partial x} + \frac{\partial u_1}{\partial x}\right) + \frac{\mathrm{d}u_0}{\mathrm{d}y}(\varepsilon V_1 + v_1) \\ &\quad = -\frac{\partial p_1}{\partial x} - \Delta\frac{\partial P_1}{\partial x} + \varepsilon\left(\frac{\partial^2 U_1}{\partial Y^2} + \varepsilon^2\frac{\partial^2 u_1}{\partial y^2}\right) + \mathrm{O}(\varepsilon^3) \end{aligned} \tag{19b}$$

$$\begin{aligned} &\varepsilon\left[(U_1 + u_1)\left(\varepsilon\frac{\partial V_1}{\partial x} + \frac{\partial v_1}{\partial x}\right) + (\varepsilon V_1 + v_1)\left(\frac{\partial V_1}{\partial Y} + \frac{\partial v_1}{\partial y}\right)\right] + u_0\left(\varepsilon\frac{\partial V_1}{\partial x} + \frac{\partial v_1}{\partial x}\right) \\ &\quad = -\frac{\partial p_1}{\partial y} - \Delta\varepsilon^{-1}\frac{\partial P_1}{\partial Y} + \varepsilon^2\left(\frac{\partial^2 V_1}{\partial Y^2} + \varepsilon\frac{\partial^2 v_1}{\partial y^2}\right) + \mathrm{O}(\varepsilon^3) \end{aligned} \tag{19c}$$

At this point of the discussion, it is important to stress that the objective is to construct a uniformly valid approximation of the flow characteristics. Then, we try to simplify the above equations so as to obtain equations valid everywhere in the flow field and not only in the boundary layers.

To simplify the equations, it is necessary to take into account the singular behaviour of u_1 and v_1 and their y-derivatives when $y \to -\frac{1}{2}$. In order to ensure that the behaviour of the sought approximation for u and v is bounded, this leads to keep terms which are apparently negligible. In particular, using (11a), we have

$$\varepsilon^3\frac{\partial^2 u_1}{\partial y^2} = 2\frac{p_{10}}{Y^2}\varepsilon$$

so that this term is of order ε in the boundary layer.

Another point is the determination of the pressure gauge Δ. From the condition on the transverse velocity given by (16a) and from (10c), in the boundary layer, we have $v_1 = \mathrm{O}(\varepsilon)$ and $\frac{\partial p_1}{\partial y} = \mathrm{O}(\varepsilon^2)$. Then, from (19c), we must take $\Delta = \mathrm{O}(\varepsilon^3)$, otherwise the transverse momentum equation cannot be satisfied.

Finally, neglecting $O(\varepsilon^3)$ terms in (19b), and coming back to approximations (u, v, p) expressed by (17a)–(17c), the simplified form of (19a)–(19b) is

$$\frac{\partial u}{\partial x} + \frac{\partial v}{\partial y} = 0 \tag{20a}$$

$$\varepsilon\left(u\frac{\partial u}{\partial x} + v\frac{\partial u}{\partial y}\right) + u_0\frac{\partial u}{\partial x} + v\frac{\mathrm{d}u_0}{\mathrm{d}y} = -\frac{\partial p_1}{\partial x} + \frac{1}{\mathcal{R}}\frac{\partial^2 u}{\partial y^2} \tag{20b}$$

Of course, the same equations are obtained if we consider the contribution of the upper boundary layer.

It must be noted that (20a)–(20b) are valid everywhere in the flow field. In particular, in the core of the flow, these equations reduce to (9a)–(9b) up to the term $\frac{1}{\mathcal{R}}\frac{\partial^2 u}{\partial y^2}$ which is $O(\varepsilon^3)$ in the core. Eqs. (20a)–(20b) are used to calculate the velocity components (u, v) in the whole flow field which are close to the velocity components (u_1, v_1) in the core. In addition, the determination of the pressure p_1 requires the use of the core flow equations. Finally, the generalized boundary layer equations (20a)–(20b) must be solved in association with the core flow equations and the flow field solution (u, v) is an *approximation valid in the whole channel*.

5. Global IBL model

The generalized asymptotic expansions for the velocity components are given by

$$v_{(x)} = u_0(y) + \varepsilon u(x, y, \varepsilon) + \cdots \tag{21a}$$

$$v_{(y)} = \varepsilon v(x, y, \varepsilon) + \cdots \tag{21b}$$

where (u, v) is the preceding uniformly valid approximation. If we set

$$\tilde{u} = u_0 + \varepsilon u \tag{22a}$$

$$\tilde{v} = \varepsilon v \tag{22b}$$

$$\tilde{p}_1 = -\frac{2x}{\mathcal{R}} + \varepsilon p_1 + p_c \tag{22c}$$

where p_c is an arbitrary constant, (20a)–(20b) become

$$\frac{\partial \tilde{u}}{\partial x} + \frac{\partial \tilde{v}}{\partial y} = 0 \tag{23a}$$

$$\tilde{u}\frac{\partial \tilde{u}}{\partial x} + \tilde{v}\frac{\partial \tilde{u}}{\partial y} = -\frac{\partial \tilde{p}_1}{\partial x} + \frac{1}{\mathcal{R}}\frac{\partial^2 \tilde{u}}{\partial y^2} \tag{23b}$$

Eqs. (23a)–(23b) have the same form as Prandtl's equations, but they are valid everywhere in the flow field and the pressure is not constant in the y-direction.

With the change of variables

$$\tilde{u}_1 = u_0 + \varepsilon u_1 \tag{24a}$$

$$\tilde{v}_1 = \varepsilon v_1 \tag{24b}$$

the core flow equations, in their nonlinear form (9a)–(9c), are

$$\frac{\partial \tilde{u}_1}{\partial x} + \frac{\partial \tilde{v}_1}{\partial y} = 0 \tag{25a}$$

$$\tilde{u}_1\frac{\partial \tilde{u}_1}{\partial x} + \tilde{v}_1\frac{\partial \tilde{u}_1}{\partial y} = -\frac{\partial \tilde{p}_1}{\partial x} + \frac{1}{\mathcal{R}}\frac{\mathrm{d}^2 u_0}{\mathrm{d}y^2} \tag{25b}$$

$$\tilde{u}_1\frac{\partial \tilde{v}_1}{\partial x} + \tilde{v}_1\frac{\partial \tilde{v}_1}{\partial y} = -\frac{\partial \tilde{p}_1}{\partial y} \tag{25c}$$

The full global IBL model is made of (23a)–(23b) and (25a)–(25c). The two sets of equations are coupled through the pressure and must be solved simultaneously. Altogether, these equations provide us with a uniformly valid approximation for the velocity components $\tilde{u}$, $\tilde{v}$ and for the pressure.

Boundary conditions are required. The complete discussion of this question and of the solution procedure is given in Section 6.1 for a simplified pressure law and in Sections 7.1–7.2 for a linearized version of the model.

Firstly, at the walls, the condition of zero velocity applies

$$y = y_l: \quad \tilde{u} = 0, \quad \tilde{v} = 0 \tag{26a}$$

$$y = y_u: \quad \tilde{u} = 0, \quad \tilde{v} = 0 \tag{26b}$$

Secondly, in Sections 6.1 and 7.1 it is shown that an additional condition is required to solve the core flow equations. This condition is obtained by arguing that, in the core flow, the solutions given by the generalized boundary layer equations and by the core flow equations must agree. This condition is implemented by writing

$$\tilde{v}(y_c) = \tilde{v}_1(y_c) \tag{27}$$

where $y = y_c$ is a line located in the core flow. As indicated in Section 6.1, (27) can be interpreted as the displacement of the core flow by the boundary layers. In [2], it is shown that the results are not very sensitive to the value of y_c as long as the line $y = y_c$ is outside the wall boundary layers.

6. Simplified method for the pressure

The pressure is at the heart of the problem formulated in Section 5, but its calculation based on the use of (25a)–(25c) is rather involved. In Section 7, it will be shown how this calculation is performed when the equations are linearized. Here, we describe a simpler approach suggested by Smith's theory [13,14]. This method has been used to produce the results presented in Section 6.2.

6.1. Simplified method and numerical procedure

A possible approximation of (10a)–(10c) consists of neglecting the pressure term in the streamwise momentum equation. Then, the core flow equations (10a)–(10c) reduce to

$$\frac{\partial u_1}{\partial x} + \frac{\partial v_1}{\partial y} = 0 \tag{28a}$$

$$u_0 \frac{\partial u_1}{\partial x} + v_1 \frac{\mathrm{d}u_0}{\mathrm{d}y} = 0 \tag{28b}$$

$$u_0 \frac{\partial v_1}{\partial x} = -\frac{\partial p_1}{\partial y} \tag{28c}$$

It can be shown [2] that this system of equations is valid for asymmetric channels with indentations whose height is of order ε and whose length is asymptotically larger than the channel height and of order $\varepsilon^{-\alpha}$ $(0 < \alpha \leqslant 1/2)$. This approximation contains the critical case of asymmetric channels in Smith's analysis with $\alpha = 1/2$ and $\varepsilon = \mathcal{R}^{-2/7}$.

With the change of variables (24a), (24b), (22c), the solution to (28a)–(28c) is

$$\tilde{u}_1 - u_0 = \tilde{A}(x) \frac{\mathrm{d}u_0}{\mathrm{d}y} \tag{29a}$$

$$\tilde{v}_1 = -\frac{\mathrm{d}\tilde{A}}{\mathrm{d}x} u_0 \tag{29b}$$

$$\tilde{p}_1 + \frac{2x}{\mathcal{R}} = \widetilde{B}(x) + \frac{\mathrm{d}^2 \tilde{A}}{\mathrm{d}x^2} \int_0^y u_0^2(\eta)\, \mathrm{d}\eta \tag{29c}$$

where η is an integration variable and the arbitrary constant in the pressure is absorbed in the function $\widetilde{B}(x)$.

The solution depends on the Reynolds number $\mathcal{R}$ which is a parameter of the solution. Then, the functions $\tilde{A}$ and $\widetilde{B}$ depend parametrically on $\mathcal{R}$. Strictly, we should write $\tilde{A} = \tilde{A}(x; \mathcal{R})$ and $\widetilde{B} = \widetilde{B}(x; \mathcal{R})$. Here, the numerical solution is determined for a given Reynolds number and the dependence of $\tilde{A}$ and $\widetilde{B}$ on $\mathcal{R}$ is omitted.

With Poiseuille flow solution for u_0, the pressure is given by

$$\tilde{p}_1 + \frac{2x}{\mathcal{R}} = \widetilde{B}(x) + \frac{\mathrm{d}^2\tilde{A}}{\mathrm{d}x^2}\left(\frac{y}{16} - \frac{y^3}{6} + \frac{y^5}{5}\right) \tag{30}$$

Finally, the simplified global IBL model is made of (23a)–(23b) and (30).

In this formulation, the question is to determine the function $\widetilde{B}(x)$ and the so-called *displacement function* $\tilde{A}(x)$. To this end, two conditions are used. The first one is to ensure mass flow conservation in the channel and the second one is given by (27).

The numerical solution is obtained as described below. A step by step marching procedure from upstream to downstream is used to calculate $\tilde{u}$ and $\tilde{v}$ from (23a)–(23b). Several sweeps of the calculation domain are required in order to take into account the upstream influence. At a given station, as a first approximation, it is assumed that the function $\tilde{A}(x)$ is known. The solution of the generalized boundary layer equations is determined by iterating on the value of function $\widetilde{B}$ at the considered station in order to ensure global mass flow conservation in the channel, i.e. to satisfy $\tilde{v} = 0$ on both walls. More precisely, the derivative $\frac{\mathrm{d}\widetilde{B}}{\mathrm{d}x}$, which is present in the momentum equation, is determined. Upon convergence, an updated value of $\tilde{A}$ is calculated as follows. The integration of the continuity equation gives

$$\int_{y_l}^{y_c} \frac{\partial\tilde{u}}{\partial x}\,\mathrm{d}y + [\tilde{v}]_{y_l}^{y_c} = 0 \tag{31}$$

where y_c is an arbitrary line in the core flow. Taking into account (27) and the wall condition $\tilde{v}(y_l) = 0$, we obtain

$$\int_{y_l}^{y_c} \frac{\partial\tilde{u}}{\partial x}\,\mathrm{d}y + \tilde{v}_1(y_c) = 0 \tag{32}$$

With (29b), the updated value of the displacement function $\tilde{A}$ is given by

$$\frac{\mathrm{d}\tilde{A}}{\mathrm{d}x} = \frac{1}{u_0(y_c)}\int_{y_l}^{y_c} \frac{\partial\tilde{u}}{\partial x}\,\mathrm{d}y \tag{33}$$

This equation shows that (27) expresses the displacement of the core flow by the boundary layers.

When the updated value of $\tilde{A}$ is determined, the calculations proceed to the next station. The updated value of $\tilde{A}$ is used at the next sweep. In order to ensure the convergence of the successive sweeps, an underrelaxation on $\tilde{A}$ is necessary.

Another point is the discretization of the pressure term in (23b), which is important to reproduce the upstream influence [11]. The derivative $\frac{\mathrm{d}\tilde{A}}{\mathrm{d}x}$ is calculated by means of (33) and we discretize the quantity $\frac{\mathrm{d}^3\tilde{A}}{\mathrm{d}x^3}$ to express $\frac{\partial\tilde{p}_1}{\partial x}$ from (30). To evaluate the second derivative of $\frac{\mathrm{d}\tilde{A}}{\mathrm{d}x}$, we use a five point stencil, with one point upstream and three points downstream of the calculated station.

6.2. Comparison with Navier–Stokes solutions

In order to assess the validity of the proposed global IBL model, comparisons with Navier–Stokes solutions are presented in this subsection. The Navier–Stokes solutions were obtained by Dechaume who developed a highly accurate solver [3]. A spectral method based on Legendre polynomials has been implemented and the solution involves a domain decomposition of Dirichlet–Neuman type. A technique of velocity–pressure decoupling is used. For the time integration, the time derivatives are expressed by an implicit Euler scheme, the nonlinear terms and the pressure boundary conditions are extrapolated. The resulting linear systems are solved by successive diagonalizations.

For these comparisons, the flow is calculated in a channel whose upper wall is flat and the lower wall is deformed in the domain $-L/2 \leqslant x \leqslant L/2$ according to

$$y_l = -\frac{1}{2} + \frac{h}{2}\left[1 + \cos\left(\frac{2\pi x}{L}\right)\right] \tag{34}$$

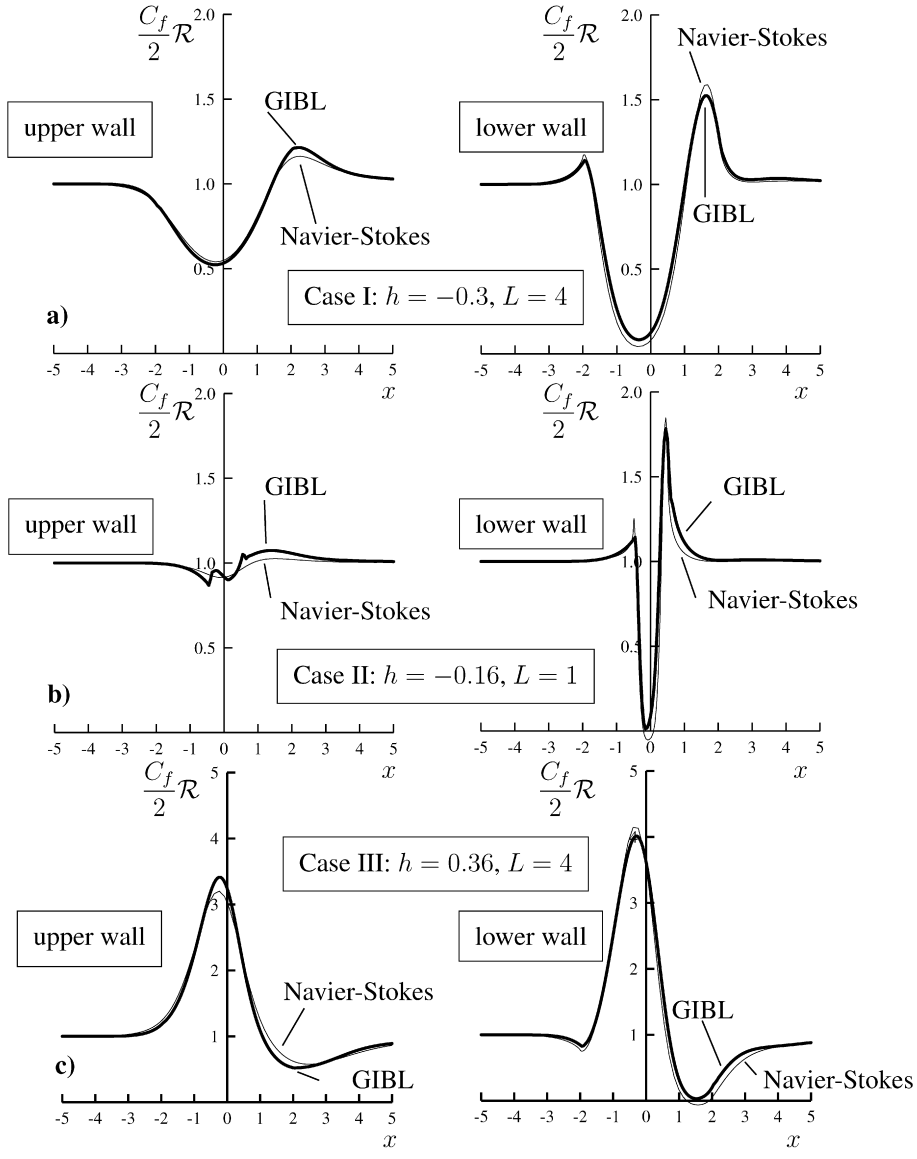

Fig. 2. Comparisons between GIBL and NS solutions.

Outside the domain $-L/2 \leqslant x \leqslant L/2$, the lower wall is flat. In (34), y_l, x and L are nondimensionalized with the width H^* of the nondeformed channel.

Three cases have been selected:

Case I

$$h = -0.3, \quad L = 4, \quad \mathcal{R} = 1000 \tag{35}$$

Case II

$$h = -0.16, \quad L = 1, \quad \mathcal{R} = 1000 \tag{36}$$

Case III

$$h = 0.36, \quad L = 4, \quad \mathcal{R} = 1000 \tag{37}$$

In the first two cases, the lower wall is deformed by a trough, and in the third case, the lower wall is deformed by a bump. The characteristics of the wall indentations were chosen to produce a flow which is close to separation somewhere on the lower wall. For all cases, the flow was calculated in a domain much longer than the wall deformation so that a nonperturbed flow is recovered at the inlet and outlet sections.

Using the definition of the skin-friction coefficient

$$C_f = \frac{2}{\mathcal{R}} \frac{\partial \tilde{u}}{\partial y}\bigg|_{y=y(\text{wall})} \tag{38}$$

the evolution of $\frac{C_f}{2}\mathcal{R}$ is plotted as function of x in Figs. 2(a)–2(c). The overall agreement between the global IBL results and the Navier–Stokes solutions is very satisfactory. Considering that the Navier–Stokes results are reference solutions, the shape of the curves and the level of the skin-friction are well predicted by the global IBL model.

In the case of the shorter trough ($L = 1$, $h = -0.16$), Case II, the global IBL model leads to a very irregular evolution of the skin-friction on the upper wall whereas the Navier–Stokes solution is smooth. This case is on the limit of validity of the global IBL model. These wiggles can be due to the law (30) which is too simple to reproduce the pressure in a cross-section or to the generalized boundary layer equations which are a too drastic simplification of Navier–Stokes equations. The origin of the problem cannot be ascertained. In any case, the amplitude of the wiggles is small and this failure does not alter the general behaviour of the results.

As noted by Lagrée et al. [7], the perturbation is weaker on the flat wall than on the opposite wall but this asymmetry effect is less pronounced when the wall deformation is very long. When the wall deformation is long enough, the cross-section pressure variations are very small and it is sufficient to assume that $\frac{\partial p}{\partial y} = 0$. For more severe wall deformations, the hypothesis of a constant pressure in a cross-section does not hold.

Two final remarks are made below. First, results produced by the present method have been compared favourably with Smith's theory [2]. This means that the two theories are consistent. Moreover, it can be shown theoretically that our approach contains Smith's theory. Second, the pressure law (30) is established for large Reynolds numbers and for wall indentations whose height is small and length is large compared to the channel width. Even if these conditions are not satisfied a priori in the test cases, the agreement of the present results with Navier–Stokes solutions is strikingly good.

7. Linearized global IBL model

7.1. Description of the model

In order to evaluate the effects of the pressure law, another simplified model has been studied. It is assumed that the wall perturbations are small enough to neglect the quadratic terms in (20b). The so obtained model is the linearized version of the complete model presented in Section 5.

With the flow decomposition given by (22a)–(22c) and (24a)–(24b), the equations for the flow perturbations u, v are

$$\frac{\partial u}{\partial x} + \frac{\partial v}{\partial y} = 0 \tag{39a}$$

$$u_0 \frac{\partial u}{\partial x} + v \frac{\mathrm{d}u_0}{\mathrm{d}y} = -\frac{\partial p_1}{\partial x} + \frac{1}{\mathcal{R}} \frac{\partial^2 u}{\partial y^2} \tag{39b}$$

Eqs. (10a)–(10c), which are valid in the core, can be replaced by Poisson's equation for v_1 obtained by eliminating the pressure

$$u_0 \left(\frac{\partial^2 v_1}{\partial x^2} + \frac{\partial^2 v_1}{\partial y^2} \right) - \frac{\mathrm{d}^2 u_0}{\mathrm{d}y^2} v_1 = 0 \tag{40}$$

It must be noted that the linearization of equations does not mean that the wall indentations are long enough to neglect the term $\frac{\partial p_1}{\partial x}$ in the core flow x-momentum equation. The pressure variations are not ruled by (30). Using the continuity

equation (10a), the x-momentum equation yields

$$-\frac{\partial p_1}{\partial x} = -u_0 \frac{\partial v_1}{\partial y} + v_1 \frac{\mathrm{d}u_0}{\mathrm{d}y} \tag{41}$$

Finally, the model is made of (39a)–(39b) and (40). In (39b), the x-component of the pressure gradient is obtained from (41).

Boundary conditions are required. At the walls, the conditions of zero velocity are valid. As the model is linearized, these conditions are not applied exactly at the walls but are transferred to the lines $y = -1/2$ and $y = 1/2$. With the walls equations (5), along the lower wall for example, a Taylor series expansion is applied to the exact boundary conditions (26a) and, with the condition $\frac{\mathrm{d}u_0}{\mathrm{d}y} = 1$ at $y = -\frac{1}{2}$, we obtain

$$u\left(x, -\frac{1}{2}\right) = -F \tag{42a}$$

$$v\left(x, -\frac{1}{2}\right) = 0 \tag{42b}$$

In the same manner, for the upper wall, we have

$$u\left(x, \frac{1}{2}\right) = -G \tag{43a}$$

$$v\left(x, \frac{1}{2}\right) = 0 \tag{43b}$$

Roughly speaking, it can be said that, for a given pressure gradient, the generalized boundary layer equations need three boundary conditions in the y-direction. On the other hand, Poisson's equation needs two boundary conditions in the y-direction. Only four boundary conditions coming from the condition of zero velocity at the walls have been explicited. The missing condition is (27) which gives

$$v(x, y_c) = v_1(x, y_c) \tag{44}$$

Finally, the linearized equations (39a)–(39b), (40) and (41) are solved in a rectangle bounded by the lines $y = -\frac{1}{2}$ and $y = \frac{1}{2}$ and by an inlet and an outlet sections. The inlet and outlet sections are chosen sufficiently far away from the wall indentations in order to have negligible perturbations in these sections.

The numerical procedure used to solve the equations and to satisfy the boundary conditions is explained in the next subsection.

7.2. Numerical procedure

Poisson's equation (40) for v_1 is discretized using a five-point stencil. A successive line overrelaxation method is applied to solve the resulting equations. According to this technique, an iterative procedure is implemented in which the calculation domain is swept from upstream to downstream. When the solution is calculated at a given x-station, the value of v_1 at the upstream x-station is the updated value of v_1 calculated at the current iteration whereas the value of v_1 at the downstream station is taken at the previous iteration. The sweeping of the calculation domain is repeated until convergence is achieved.

At a given x-station, the longitudinal component of the pressure gradient is calculated from (41) and is used to solve the generalized boundary layer equations. These equations are discretized using a standard finite difference method with three points in the y-direction and two points in the x-direction.

In fact, Poisson's equation and the generalized boundary layer equations are strongly coupled and the whole set of equations is solved as simultaneously as possible. The procedure is described below.

The calculation of the values of u, v and v_1 at the different grid points for a given x-station consists of solving a system of algebraic equations in which the coefficients of the unknowns form tridiagonal matrices. The main problem is that the values of v_1 are not known a priori along the lines $y = -1/2$ and $y = 1/2$.

At a given x-station, the solution of Poisson's equation can be written as

$$v_{1i} = A_i v_1\left(-\frac{1}{2}\right) + B_i v_1\left(\frac{1}{2}\right) + C_i \tag{45}$$

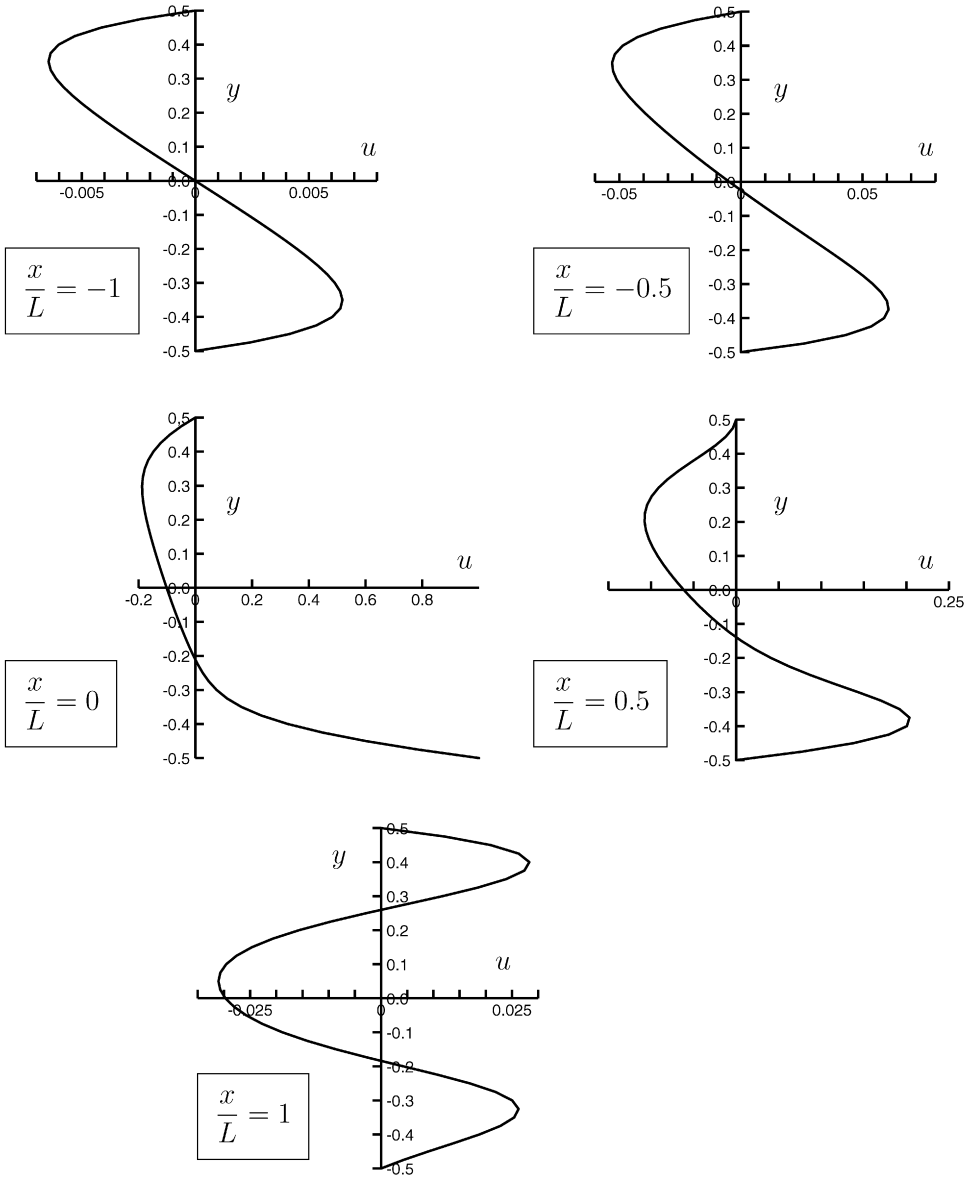

Fig. 3. Evolution of the u-component of velocity. The channel wall indentations are defined by (49a) and (49b) with $L = 2$. The Reynolds number is $\mathcal{R} = 1000$.

where v_{1i} is the value of v_1 at a certain grid point i along a line x = const. The coefficients A_i, B_i and C_i do not depend on the values $v_1(-1/2)$ and $v_1(1/2)$ and are calculated explicitly.

In the same way, after replacing the component $\frac{\partial p_1}{\partial x}$ by its expression as a function of v_1 and of its transverse derivative, the solution of the generalized boundary layer equation for u has the form

$$u_i = a_i v_1\left(-\frac{1}{2}\right) + b_i v_1\left(\frac{1}{2}\right) + c_i \tag{46}$$

and for v, we have

$$v_i = \alpha_i v_1\left(-\frac{1}{2}\right) + \beta_i v_1\left(\frac{1}{2}\right) + \gamma_i \tag{47}$$

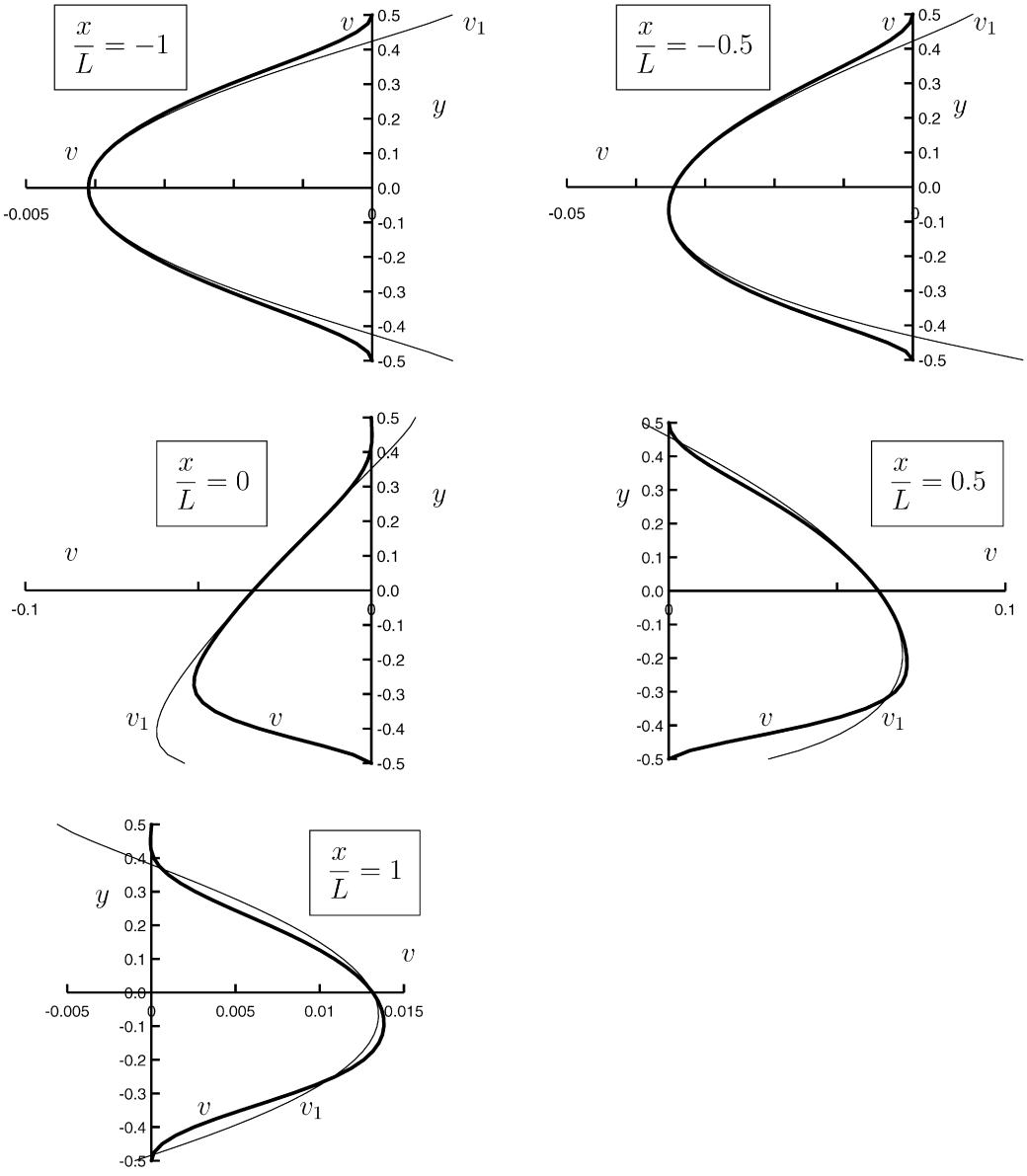

Fig. 4. Evolution of the v-component of velocity. The channel wall indentations are defined by (49a) and (49b) with $L = 2$. The Reynolds number is $\mathcal{R} = 1000$.

Solution (46) for u is obtained by applying the wall conditions on u. This means that the coefficients a_i, b_i and c_i are calculated by taking into account these boundary conditions. For v, the above solution (47) is obtained by using the condition $v = 0$ along one wall only, for example the lower wall. Indeed, only one boundary condition can be taken into account because v is deduced from u by integrating the continuity equation which is of first order with respect to the transverse coordinate.

At this stage, two conditions are not yet prescribed. The first condition is $v = 0$ along the other wall (the upper wall); this condition is equivalent to the prescription of a constant mass flow in the whole channel. The second condition is the coupling between the boundary layer solution and the core flow solution expressed by (44). These two missing conditions are written from the expressions of v_{1i}, u_i and v_i. For example, the coupling condition writes

$$A_c v_1\left(-\frac{1}{2}\right) + B_c v_1\left(\frac{1}{2}\right) + C_c = \alpha_c v_1\left(-\frac{1}{2}\right) + \beta_c v_1\left(\frac{1}{2}\right) + \gamma_c \tag{48}$$

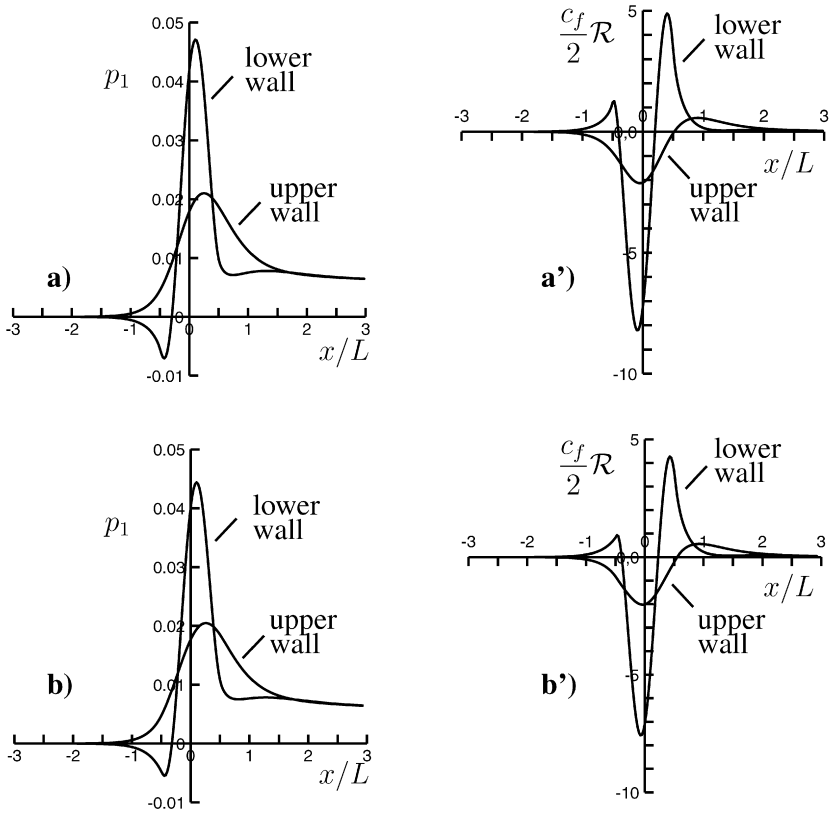

Fig. 5. Evolutions of the perturbations of the wall pressure and of the skin-friction along the lower and upper walls, $\mathcal{R} = 1000$, $L = 2$. Figures (a) and (a′) correspond to the linearized method described in Section 7.1. Figures (b) and (b′) correspond to a linearized version of the method described in Section 6.1.

where the index c denotes the given core line. Eq. (48) gives a first relation to calculate the values of $v_1(-1/2)$ and $v_1(1/2)$. The second relation is obtained by calculating the mass flow from the expression of u_i (46).

When the values of $v_1(-1/2)$ and $v_1(1/2)$ are determined, the solutions for v_{1i}, u_i and v_i are known from (45)–(47) and the calculation can proceed to the next x-station. In this way, the whole domain is swept from upstream to downstream. The sweep is repeated until convergence is achieved.

This procedure ensures a quasi-simultaneous resolution of the whole system of equations and makes the algorithm very efficient [18].

7.3. Results

The linearized method presented in Section 7.1 is applied to the calculation of the flow in a channel whose walls are defined by

$$F = -\frac{1}{2}\left[1 + \cos\left(\frac{2\pi x}{L}\right)\right] \quad \text{if } -\frac{1}{2} \leqslant \frac{x}{L} \leqslant \frac{1}{2} \tag{49a}$$

$$G = 0 \tag{49b}$$

Outside the domain $-1/2 \leqslant x/L \leqslant 1/2$, the lower wall is flat. The upper wall is flat all along the channel.

The results presented below have been obtained for a Reynolds number $\mathcal{R} = 1000$.

In Figs. 3 and 4 the profiles of the velocity components u and v are shown at a few selected stations for a lower wall indentation defined by $L = 2$. The velocity components u and v are the flow perturbations as defined by (22a) and (22b). In Fig. 4, the velocity component v calculated from the generalized boundary layer equations (39a)–(39b) is compared to the velocity component v_1 calculated from the core flow equation (40). In the core, a good agreement

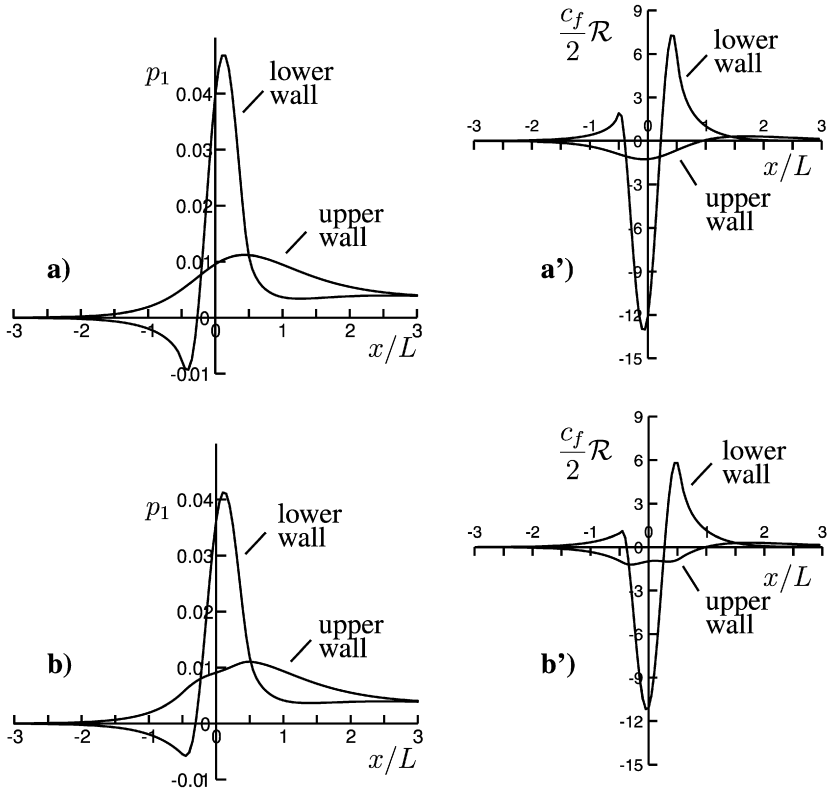

Fig. 6. Evolutions of the perturbations of the wall pressure and of the skin-friction along the lower and upper walls, $\mathcal{R} = 1000$, $L = 1$. Figures (a) and (a′) correspond to the linearized method described in Section 7.1. Figures (b) and (b′) correspond to a linearized version of the method described in Section 6.1.

between v and v_1 is observed even if v_1 is not symmetrical (by contrast, v_1 is symmetrical in the critical case of Smith's theory). Let us recall that condition (44) is applied along a core line $y = y_c$. Here, the chosen core line is $y = 0$, but any other line would give very close results as far as the line $y = y_c$ is not located in the wall boundary layers. In the core, the agreement between v and v_1 is better if the term $\frac{1}{\mathcal{R}}\frac{\partial^2 u}{\partial y^2}$ in (39b) is smaller. This means that the hypothesis of an inviscid core is well justified if the Reynolds number is large and if the curvature of the velocity profile u is small. Indeed, it has been observed that the agreement between v and v_1 deteriorates if the curvature of the velocity profile u becomes large.

The evolutions of the perturbations of the wall pressure and of the skin-friction for two wall indentations are shown in Fig. 5 for $L = 2$ and in Fig. 6 for $L = 1$. The results presented in figures (a) and (a′) are obtained with the linearized method described in Section 7.1 whereas the results presented in figures (b) and (b′) correspond to a linearized version of the method described in Section 6.1.

The perturbations are not restricted to the domain of the wall indentation $-1/2 \leqslant x/L \leqslant 1/2$. The flow is perturbed downstream but also upstream of the indentation. This upstream effect is visible for the two cases $L = 2$ and $L = 1$ but it is more pronounced for the case $L = 1$ which is a more severe indentation than the case $L = 2$ for the same indentation height.

The pressure peak on the lower wall is of the same order for $L = 1$ and $L = 2$ but the pressure varies on a shorter distance for the case $L = 1$. Then, the variation of the skin-friction is larger for the case $L = 1$. The minimum value of the reduced skin-friction perturbation is around -8 for $L = 2$ and around -12 for $L = 1$.

We note that the pressure perturbation is larger on the upper surface for $L = 2$. When the length of the wall indentation increases, the pressure distributions on the lower and upper walls tend to be equal. It is as if the channel became symmetrical.

For the case $L = 1$, the linearized version of the method described in Section 6.1 leads to wiggles in the distribution of pressure and of skin-friction on the upper wall. The same problem observed in Fig. 2 was discussed at the end of Section 6.2. On the contrary, the linearized method of Section 7.1 gives very smooth results on the upper wall. It is believed that this method in which the core flow is calculated from Poisson's equation (40) is more accurate than the method in which the pressure is calculated from (30).

8. Conclusion

Different models of the flow at high Reynolds number in a channel with deformed walls have been constructed. Their solutions represent a good approximation of the solution of Navier–Stokes equations. The so-called Successive Complementary Expansion Method, SCEM, used to develop these models is relatively recent as far as generalized asymptotic expansions are involved. This method is particularly well adapted to flows in which a strong coupling exists between inviscid and viscous regions. An interesting idea is that the form of the uniformly valid approximation is assumed. This assumption is a good alternative to the well known method of matched asymptotic expansion and avoids the difficulty of an asymptotic matching process. The flow in a channel is particularly interesting because the solution of the Eulerian perturbation in the core is singular near the walls. Obviously, the uniformly valid approximations obtained with our analysis are not singular. In Smith's theory, which is the analogue for internal flow of the triple deck theory, the perturbations of streamwise and transverse velocity components in the core are respectively antisymmetrical and symmetrical. It is clear that, for the Reynolds number and the size of wall deformations considered here, the usual hypotheses of asymptotic analysis are not really satisfied. Here, the core flow velocity perturbations do not have the symmetry properties given above. Nevertheless, thanks to the employed method, even in the case of the linearized model, convincing results are obtained as shown by the comparisons with Navier–Stokes solutions.

References

[1] J. Cousteix, J. Mauss, Approximations of the Navier–Stokes equations for high Reynolds number flows past a solid wall, J. Comp. Appl. Math. 166 (1) (2004) 101–122.
[2] J. Cousteix, J. Mauss, Asymptotic Analysis and Boundary Layers, Scientific Computation, vol. XVIII, Springer, Berlin, Heidelberg, 2007.
[3] A. Dechaume, Analyse asymptotique et numerique des equations de Navier–Stokes: cas du canal, Ph.D. thesis, Universite Paul Sabatier, Toulouse, 2006.
[4] A. Dechaume, J. Cousteix, J. Mauss, An interactive boundary layer model compared to the triple deck theory, Eur. J. Mech. B Fluids 24 (2005) 439–447.
[5] P. Lagrée, E. Berger, M. Deverge, C. Vilain, A. Hirschberg, Characterization of the pressure drop in a 2d symmetrical pipe: some asymptotical, numerical and experimental comparisons, ZAMM Z. Angew. Math. Mech. 85 (1) (2005) 1–6.
[6] P. Lagrée, S. Lorthois, The RNS/Prandtl equations and their link with other asymptotic descriptions: Application to the wall shear stress in a constricted pipe, Int. J. Engrg. Sci. 43 (2005) 352–378.
[7] P. Lagrée, A. van Hirtum, X. Pelorson, Asymmetrical effects in a 2d stenosis, Eur. J. Mech. B Fluids 26 (2007) 83–92.
[8] M. Lighthill, On boundary-layer and upstream influence: II. Supersonic flows without separation, Proc. R. Soc. Ser. A 217 (1953) 478–507.
[9] A. Messiter, Boundary-layer flow near the trailing edge of a flat plate, SIAM J. Appl. Math. 18 (1970) 241–257.
[10] V. Neyland, Theory of laminar boundary-layer separation in supersonic flow, Izv. Akad. Nauk SSSR Mekh. Zhidk. Gaza 4 (1969) 53–57. English transl., Fluid Dynam. 4 (4), 33–35.
[11] A. Rothmayer, F. Smith, Numerical solution of two-dimensional, steady triple-deck problems, in: R.W. Johnson (Ed.), The Handbook of Fluid Dynamics, CRC Press/Springer-Verlag, Boca Raton, FL/Heidelberg, Germany, 1998, pp. 1–26 (Chapter 25).
[12] S. Saintlos, J. Mauss, Asymptotic modelling for separating boundary layers in a channel, Int. J. Engrg. Sci. 34 (2) (1996) 201–211.
[13] F. Smith, Flow through constricted or dilated pipes and channels: part 1, Quart. J. Mech. Appl. Math. XXIX (Pt 3) (1976) 343–364.
[14] F. Smith, Flow through constricted or dilated pipes and channels: part 2, Quart. J. Mech. Appl. Math. XXIX (Pt 3) (1976) 365–376.
[15] F. Smith, On the high Reynolds number theory of laminar flows, IMA J. Appl. Math. 28 (3) (1982) 207–281.
[16] I. Sobey, Introduction to Interactive Boundary Layer Theory, Oxford Applied and Engineering Mathematics, Oxford University Press, Oxford, 2000.
[17] K. Stewartson, P. Williams, Self induced separation, Proc. Roy. Soc. A 312 (1969) 181–206.
[18] A. Veldman, Matched asymptotic expansions and the numerical treatment of viscous-inviscid interaction, J. Engrg. Math. 39 (2001) 189–206.